Assessment of Coolant-Salt Solidification Under Load-Following Operation for a Marine MSR-sCO_2 System

Jeong Min Baek, Gihyeon Kim, Seungkyu Lee, Jeong Ik Lee *
Dept. Nuclear & Quantum Eng., KAIST, 291 Daehak-ro, Yuseong-Gu, Daejeon 34141, Republic of Korea
**Corresponding author: jeongiklee@kaist.ac.kr*

Keywords : Molten Salt Reactor (MSR), sCO_2 Brayton Cycle, Load-Following, Solidification

1. Introduction

Maritime transport accounts for a significant portion of global carbon emissions. The International Maritime Organization has set the goal of eliminating carbon emissions from ships by 2050. Achieving this target requires a transition from conventional diesel-based propulsion systems to carbon-neutral alternatives.

Nuclear propulsion offers a promising solution because it produces no carbon emissions and enables long-duration operation. Among nuclear technologies, the molten salt reactor (MSR) is attractive for marine applications due to its long refueling interval, high outlet temperature, and inherent safety features. These characteristics enhance efficiency compared to pressurized water reactors and align with the operational demands of maritime environments. The limited space available on ships remains a major challenge because the reactor itself cannot be substantially reduced in size. Compact power conversion systems are therefore critical for practical deployment.

The supercritical carbon dioxide (sCO_2) Brayton cycle achieves both high thermal efficiency and a compact system footprint. It is advantageous over steam Rankine and air Brayton cycles for marine propulsion. Marine operations involve frequent and rapid load changes during activities such as port entry and canal passage. Robust load-following capability is therefore required.

In MSR-sCO_2 systems, load-following operation leads to continuous variations in the properties of CO_2. When the CO_2 temperature decreases, the coolant-salt outlet temperature at the intermediate heat exchanger (IHX) can fall below its melting point, which raises the risk of solidification and challenges stable operation.

This study evaluates the load-following performance and the risk of coolant-salt solidification with respect to coolant-salt flow conditions in an MSR-sCO_2 system. The results provide essential insights for the design and commercialization of nuclear-powered marine propulsion.

2. Methods and Results

2.1 Target Reactor System

This study adopts the maritime MSFR core proposed by Go et al. as the reference model [1]. The core uses a chloride fuel salt, NaCl-KCl-UCl_3 with a composition of 42.9-20.3-36.8 mol%, an inlet temperature of 570℃, an outlet temperature of 650℃, and a fuel-salt melting point of 470.15℃. The design thermal power is 100MW_{th} and the target application is a 10,000 TEU-class vessel.

Using this core as the boundary condition, the secondary coolant loop is configured with a chloride coolant-salt to ensure chemical compatibility and straightforward integration. NaCl-KCl-$MgCl_2$ is selected in order to combine high-temperature stability with a low melting point. The lowest-melting composition of 30.2-22.7-47.1 mol% is adopted to prioritize solidification margins. Thermophysical properties and correlations are taken from the temperature-dependent relations reported by Carolina Villada et al. and the values used in this study are summarized in Table 1 [2].

Table 1: Summary of thermophysical properties of the NaCl-KCl-$MgCl_2$ (30.2-22.7-47.1 mol%) [2]

Property	**Values or correlations with T [℃]**
Melting point [℃]	$T_m = 385$
Heat capacity [J/kg· ℃]	$C_p = 1100$
Viscosity [Pa·s]	$\mu = 27.728 \times 10^{-3} \times e^{-0.00364 \times T[℃]}$
Density [kg/m³]	$\rho = 1940 - 0.42 \times T[℃]$
Thermal conductivity [W/m· ℃]	$\lambda = 0.53 - 1.32 \times 10^{-4} \times T[℃]$

Given a fuel-salt core outlet temperature of 650℃, a pinch temperature of 10℃ is applied and the coolant-salt core outlet temperature is set to 640℃. According to Williams et al., operation should maintain a margin of at least 100℃ above the coolant melting point. The selected coolant composition melts at 385℃, so the coolant-salt core inlet temperature is set to 500℃ [3].

The coolant-salt mass flow rate is determined using the adopted thermophysical properties at the coolant-salt core inlet and outlet conditions so that the loop delivers a thermal power of 100MW_{th}. The calculated value is 649.35kg/s and this reference mass flow rate is used in subsequent load-following analyses. A consolidated summary of the core and coolant loop design is provided in Table 2.

Table 2: Summary of core and coolant loop design

Reactor Thermal Power [MW_{th}]	100
Fuel-Salt Composition	NaCl-KCl-UCl_3 (42.9-20.3-36.8 mol%)
Fuel-Salt Operating Temperature [℃]	570 ~ 650
Coolant-Salt Composition	NaCl-KCl-$MgCl_2$ (30.2-22.7-47.1 mol%)
Coolant-Salt Operating Temperature [℃]	500 ~ 640
Coolant-Salt Mass Flow Rate [kg/s]	649.35

2.2. sCO_2 Cycle Design

A comparative analysis for marine applications reports that the recompression sCO_2 Brayton cycle outperforms the simple recuperated configuration in thermal efficiency and operational suitability [4]. This study therefore adopts the recompression layout and performs the cycle design using the KAIST-CCD (Closed Cycle Design) code [5]. Figure 1 presents the cycle layout and Table 3 reports the design results.

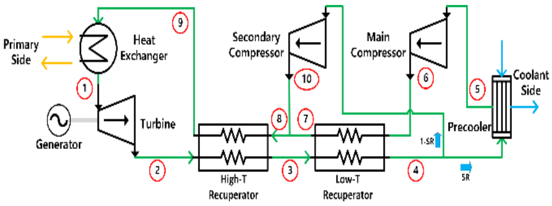

Fig. 1. Recompression Cycle Layout

Table 3: Cycle Design Results

Points	T [℃]	P [MPa]	$\dot{m}$ [kg/s]
1	630.0	19.55	558.084
2	536.97	9.46	558.084
3	216.86	9.31	558.084
4	84.83	9.16	558.084
5	40.0	9.01	396.240
6	76.18	20.0	396.240
7	201.85	19.85	396.240
8	188.95	19.85	558.084
9	485.75	19.70	558.084
10	159.24	19.85	161.844

The component design uses the temperature and pressure conditions obtained from the recompression sCO_2 Brayton cycle configured with KAIST-CCD. After fixing the operating states, these conditions are used as inputs to the component-level design.

The cycle includes four heat exchangers, namely an intermediate heat exchanger (IHX), a high-temperature recuperator (HTR), a low-temperature recuperator (LTR), and a precooler. All four heat exchangers are designed as printed circuit heat exchanger (PCHE) type using the KAIST-HXD (Heat Exchanger Design) code developed for PCHE design [6].

The turbomachinery consists of two compressors and one turbine. Their geometry and performance were designed and evaluated using the KAIST-TMD (Turbo Machinery Design) code [7].

2.3. sCO_2 Cycle Control Strategy

The control strategies for the sCO_2 cycle are diverse and each provides a different controllable load range and dynamic behavior. This study adopts a hybrid scheme that combines an IHX and turbine bypass with inventory control. Inventory control is advantageous for off-design efficiency but responds slowly and is limited by compressor surge. The bypass of the IHX and the turbine provides rapid response and a broad control range, but it entails a higher efficiency penalty than inventory control. Using this combined strategy, the study evaluates load-following performance and coolant-salt solidification risk across a set of coolant-salt flow conditions.

2.4. Quasi-Steady-State Analysis

This study uses the integrated in-house code KAIST-QCD for quasi-steady-state analysis. KAIST-QCD integrated KAIST-CCD, KAIST-HXD, and KAIST-TMD, which enables consistent recalculation of component performance and system response under off-design conditions. The analysis is organized into three scenarios in which the coolant-salt mass flow rate is set to 100, 40, and 20% of the reference flow rate of 649.35kg/s. For each scenario, load-following performance and the risk of coolant-salt solidification are evaluated while controlling the total CO_2 inventory and the bypass ratio as control variables.

A hybrid control scheme combines inventory control with a simultaneous bypass of the IHX and the turbine. The two controls are applied as needed to achieve transitions to the target power during load changes. Stable operation is enforced by maintaining a surge margin of 10% for both the main compressor and the recompressor. At low inlet mass flow rate, the turbine experiences a larger mismatch between the stator exit flow angle and the rotor inlet angle, which increases incidence and can cause higher losses or instability. For this reason, the turbine inlet mass flow rate was constrained to remain above 50% of the design value during load-following analyses.

Thermal boundaries and the solidification criterion are defined as follows. The coolant-salt temperature at the inlet of the IHX is fixed at 640℃. During load-following operation, the CO_2 temperature at the inlet of the IHX varies with the control variables, and the resulting heat transfer changes the coolant-salt temperature at the IHX outlet. Solidification is deemed to occur when the coolant-salt outlet temperature falls below the melting point of 385℃. Using these definitions and constraints, each coolant-salt flow scenario is assessed to confirm load-following performance and to evaluate the occurrence of solidification.

2.5. Load-Following Performance Analysis

The methodology and operating constraints were applied to three coolant-salt mass flow rate cases equal to 100%, 40%, and 20% of the design mass flow rate. Figure 2 presents the achievable load range for each case. Operation was confirmed from 100% down to 14.51% at the 100% coolant mass flow rate, from 76.58% down to 13.10% at the 40% coolant mass flow rate, and from 35.13% down to 8.07% at the 20% coolant mass flow rate. Further reduction in load was limited by the minimum turbine inlet mass flow rate requirement, which is at least 50% of the design mass flow rate to maintain turbine stability.

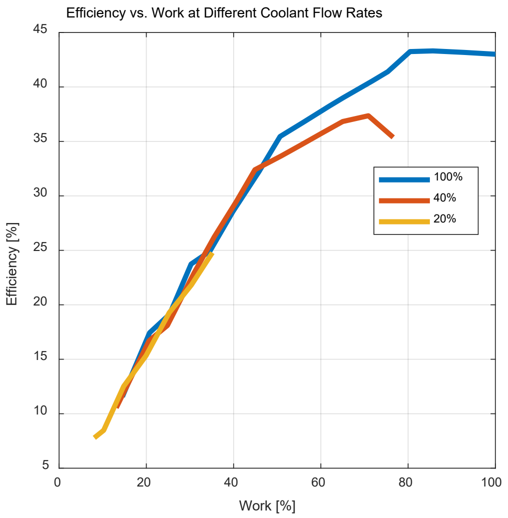

Fig. 2. Load-Following Data of Different Coolant Mass Flow Rates

Solidification risk was assessed by tracking the coolant-salt temperature at the outlet of the IHX. Figure 3 corresponds to 100% coolant-salt mass flow rate case, Figure 4 to the 40% case, and Figure 5 to the 20% case. The IHX inlet coolant-salt temperature was fixed at 640°C. As load decreased at a given coolant-salt mass flow rate, the heat transferred from the coolant-salt to the sCO_2 decreased. The temperature drop experienced by the coolant-salt across the IHX therefore became smaller, and the coolant-salt outlet temperature increased. This behavior appears in all three figures as a monotonic increase of the coolant-salt outlet temperature with decreasing load.

In the 100% coolant-salt mass flow rate case shown in Figure 3, the coolant-salt outlet temperature remained above the melting point of 385°C across the full load range, and solidification did not occur. In the 40% coolant-salt mass flow rate case shown in Figure 4, the coolant-salt outlet temperature fell below the melting point at high load because the transferred heat was large and the temperature drop on the coolant-salt side increased. As the load decreased, the transferred heat diminished, the temperature drop became smaller, and the coolant-salt outlet temperature recovered above the melting point, which avoided solidification. In the 20% coolant-salt mass flow rate case shown in Figure 5, solidification was found to be possible across the full load range. Even at low load, the very low mass flow rate produced a large temperature drop on the coolant-salt side, driving the coolant-salt outlet temperature below the melting point.

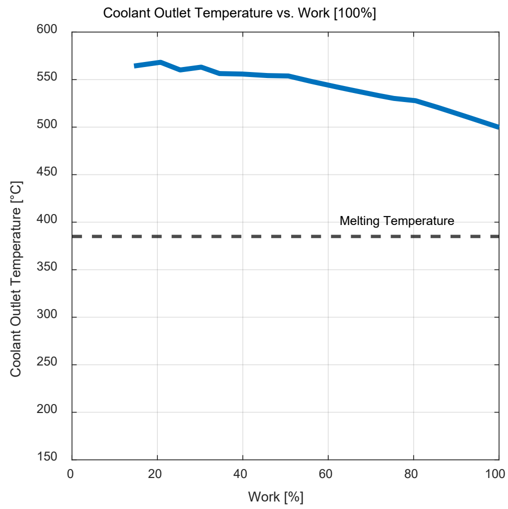

Fig. 3. Coolant Outlet Temperature of 100% Coolant Mass Flow Rate

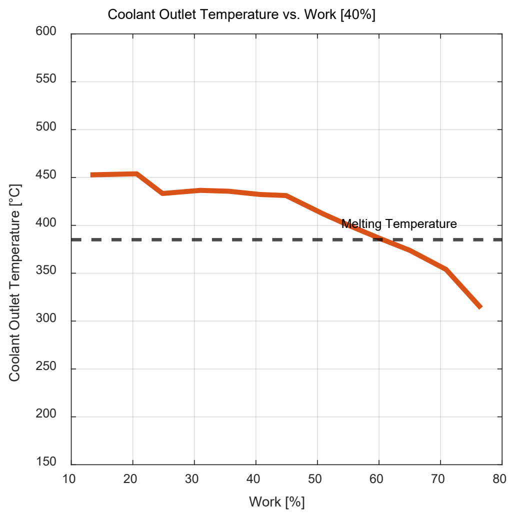

Fig. 4. Coolant Outlet Temperature of 40% Coolant Mass Flow Rate

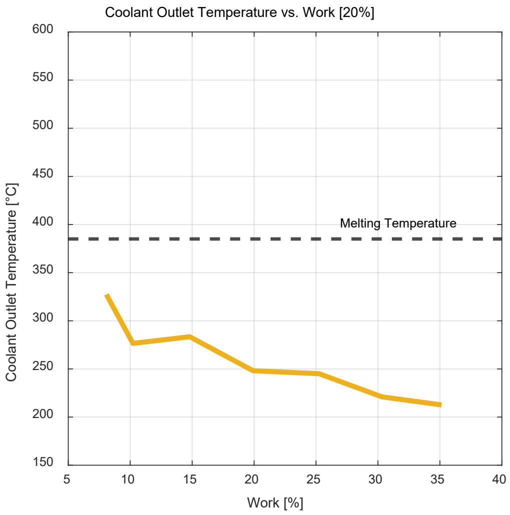

Fig. 5. Coolant Outlet Temperature of 20% Coolant Mass Flow Rate

3. Summary and Conclusions

This study quantified the interaction between load-following demands and coolant-salt solidification risk in a marine MSR–sCO_2 system. A maritime MSR was coupled to a recompression sCO_2 Brayton cycle, and a quasi-steady framework integrating KAIST-CCD, KAIST-HXD, and KAIST-TMD recalculated component and system performance consistently. Control employed inventory control together with concurrent bypass of the IHX and the turbine. A compressor surge margin of 10% was maintained, and the minimum turbine inlet mass flow rate was set to at least 50% of the design value. Thermal boundaries fixed the IHX inlet coolant-salt temperature at 640℃ and the melting point at 385℃. Three coolant-salt mass flow rate cases were analyzed for three cases: 100%, 40%, and 20% of the design value, 649.35 kg/s.

The confirmed operational envelopes were 100% down to 14.51% at 100% coolant-salt mass flow rate, 76.58% down to 13.10% at 40% coolant-salt mass flow rate, and 35.13% down to 8.07% at 20% coolant-salt mass flow rate. In every case the low-load bound was dictated by the minimum turbine inlet mass flow rate requirement. The trend shows that reduction in load requires reducing the coolant-salt mass flow rate, while maintaining a high coolant-salt mass flow rate avoids freezing but prevents further reduction in load.

Solidification risk was assessed using the coolant-salt temperature at the IHX outlet. At 100% coolant-salt mass flow rate, the outlet coolant-salt temperature remained above 385℃ across the full load range and solidification did not occur. At 40% coolant-salt mass flow rate, the coolant-salt outlet temperature fell below the melting point at high load because the transferred heat was large and the salt-side temperature drop increased, then recovered above the melting point as the load decreased. At 20% coolant-salt mass flow rate, solidification was possible across the full load range because the very low mass flow rate produced a large salt-side temperature drop even when the transferred heat was small.

These findings indicate that deep turndown is achievable only by lowering the coolant-salt mass flow rate and that this approach reduces the freeze margin. Coordinated adjustment of IHX heat duty, bypass ratio, and inventory is therefore required to preserve a safe margin while tracking marine load profiles.

Future work will be performed to quantify an alternative control that combines inventory control with turbine bypass without bypassing the IHX, with emphasis on impacts to load-following capability and solidification behavior. In parallel, design-stage analysis will be performed in which the heat exchanger is split into two stages with intermediate reheating of the coolant salt to determine whether this configuration mitigates freezing at low load.

ACKNOWLEDGEMENT

This work was supported by the National Research Foundation of Korea(NRF) grant funded by the Korea government(MSIT) (No. RS-2025-25454059).

REFERENCES

[1] Yubin Go, Tongkyu Park, Sung Kyun Zee, Jae Uk Seo, and Seong Jun Yoon, Conceptual core design study of a maritime molten salt fast reactor, Annals of Nuclear Energy, Vol.222, 2025.

[2] Carolina Villada, Wenjin Ding, Alexander Bonk, and Thomas Bauer, Engineering molten $MgCl_2$-KCl-NaCl salt for high-temperature thermal energy storage: Review on salt properties and corrosion control strategies, Solar Energy Materials and Solar Cells, Vol.232, 2021.

[3] D. F. Williams, L. M. Toth, and K. T. Clarno, Assessment of Candidate Molten Salt Coolants for the Advanced high Temperature Reactor (AHTR), 2006.

[4] Eun Sang Yun, and Jeong Ik Lee, A Study on the Layout of a Molten Salt Reactor with a Supercritical Carbon Dioxide (sCO_2) Power Conversion System Suitable for Ship Propulsion, 2025.

[5] Seongmin Son, and Jeong Ik Lee, Application of adjoint sensitivity analysis method to supercritical CO_2 power cycle optimization, Energy, Vol.147, p.1153-1164, 2018.

[6] Jinsu Kwon, and Jeong Ik Lee, Development of accelerated PCHE off-design performance model for optimizing power system control strategies in S-CO_2 power conversion system of nuclear power plant applications, Transactions of the Korean Nuclear Society Spring Meeting, 2018.

[7] Seong Kuk Cho, Jekyoung Lee, Jeong Ik Lee, and Jae Eun Cha, 1D mean Streamline Design Code Development for S-CO_2 Radial Inflow Turbine, Transactions of the Korean Nuclear Society Autumn Meeting, 2016.